Morphometrics of regmaglypts based on a 3D Model of the fusion-crusted ordinary chondrite Broek in Waterland (L6)

Veithen, L.A.V.; de Vet, S.J.

Publication date
2024

Document Version
Final published version

Published in
Proceedings of the IMC, Redu, 2023

ISBN 978-2-87355-036-3

Proceedings of the International Meteor Conference

Redu, Belgium, 2023
August 31 – September 3

Published by the International Meteor Organization
Edited by Urška Pajer and Cis Verbeeck

Proceedings of the International Meteor Conference
Redu, Belgium, August 31 – September 3, 2023
International Meteor Organization
ISBN 978-2-87355-036-3

Editing and printing:

Front cover picture: Group picture of the IMC 2023, by Peter Slansky
Publisher: The International Meteor Organization
Printed: The International Meteor Organization
Editors: Urška Pajer and Cis Verbeeck
Bibliographic records: all papers are listed with the SAO/NASA Astrophysics Data System (ADS)
http://adsabs.harvard.edu with publication code 2024pimo.conf

Distribution:

Further copies of this publication may be ordered from the International Meteor Organization, through the IMO website (http://www.imo.net).
Legal address: International Meteor Organization, Mattheessensstraat 60, 2540 Hove, Belgium.

Morphometrics of regmaglypts based on a 3D model of the fusion-crusted ordinary chondrite Broek in Waterland (L6)

Lorenz A.V. Veithen[1] and Sebastiaan J. de Vet[1,2,3]

[1] **Delft University of Technology, Aerospace Engineering, section Planetary Exploration**
l.a.v.veithen@student.tudelft.nl and s.j.devet@tudelft.nl

[2] **Meteor Section, Royal Netherlands Association for Meteorology and Astronomy (KNVWS)**
[3] **Naturalis Biodiversity Centre, Leiden**

Regmaglypts are shallow depressions on meteorite surfaces formed by ablation processes during atmospheric entry. These features can potentially offer insights in breakup events. However, quantitative methods to analyse regmaglypts have not yet been proposed to date. Here we present the results of a study to evaluate breakup processes during the luminous flight by analysing regmaglypt morphometrics. We developed a novel approach based on a 3D shape model of the Broek in Waterland meteorite that was generated using photogrammetry. We converted sections of the 3D model into a smoothed Digital Elevation Model (DEM) that contained the fracture surfaces adorned with regmaglypts. Lending techniques from terrain analyses, we extracted Land Surface Parameters (LSP) and delineated regmaglypts based on the mean curvature inflection point. The outliers of the regmaglypt population were discarded based on mean and total curvature scatter plots. The mean, profile, tangential, total and Gaussian curvatures were found to be most descriptive of regmaglypt morphologies. Various other curvature types were tested and found to be consistent across the studied regmaglypt population. Using this initial framework, we found that the two regmaglypted surfaces of the Broek in Waterland meteorite appear to be similar. This would reflect similar formative conditions, which we interpret to be most consistent with formation from the same breakup event. Future studies will aim to expand the presented method to regmaglypt populations of other L6 meteorites to understand how surface characteristics can inform us on ablation and breakup processes.

1 Introduction

Studying meteorites is a powerful way to infer key processes that contributed to solar system formation (Pfalzner et al., 2015), as it complements the understanding obtained from current architecture of the solar system, as well as knowledge gained from other planet-forming disks around young stars (Takami et al., 2013). Various meteorite classes provide insights into material types, and the geological evolution of planet-building materials (Arrol et al., 1942; Bouvier & Wadhwa, 2010; Alexander et al., 2001; Saito et al., 2020). One common class that is abundantly found amongst recovered meteorites (∼85%) on Earth are the *ordinary chondrites*. Their name stems from a key component in these rocky meteorites: *chondrules* are spherical molten droplets of a few millimetres originating from undifferentiated parent bodies (Vernazza et al., 2015; Reynolds, 2004). Like many other meteorite classes, the petrographic properties, bulk-rock characteristics and alterations histories provide insight into formation and processing of early solar system materials (Pfalzner et al., 2015). Their survival during atmospheric entry and recovery on the ground is key to obtaining such study materials.

Meteorites are delivered to Earth when dynamic resonance with Jupiter perturbs the orbit of the parent body (meteoroid or asteroid) and shifts the meteoroid perihelion inside Earth's orbit over the span of millions of years to an Earth-crossing orbit (Wisdom, 1987; Wisdom, 1985). Depending on the meteoroid orbital arrangement relative to the Earth orbital motion and the source (asteroidal vs. cometary), entry velocities can vary from 11.2 km/s to 72 km/s. During entry, the meteoroid enters the atmosphere and can be observed as a fireball when the majority of the kinetic energy is converted into heat (Romig, 1965). The high temperatures drive ablation of the meteoroid, and based on recovered meteorites this mass-loss is often 90% compared to the initial pre-atmospheric mass. In addition to the ablation processes, dynamic loading from the aerodynamic pressure can exceed the tensile strength of the material and cause fragmentation of the meteoroid (Revelle, 1979; Ceplecha & Revelle, 2005). Meteoroids with sufficient mass, or entering with favourable geometries that reduce heating can thus survive the rigours of the luminous phase and deliver remaining material to the Earth's surface in the form of meteorites.

Recovered chondrites are often covered with a fusion crust: a thin, diagnostic glassy rind on the exterior of the rock that has been created by the ablation due to the fireball's plasma (Towner et al., 2022). When the rock surface is exposed to the fireball's plasma, surface depressions are formed of different sizes and depths called regmaglypts (Botines & Ernstson, 2005). Regmaglypts and their distribution can inform us about the atmospheric (luminous) flight of a meteorite as they

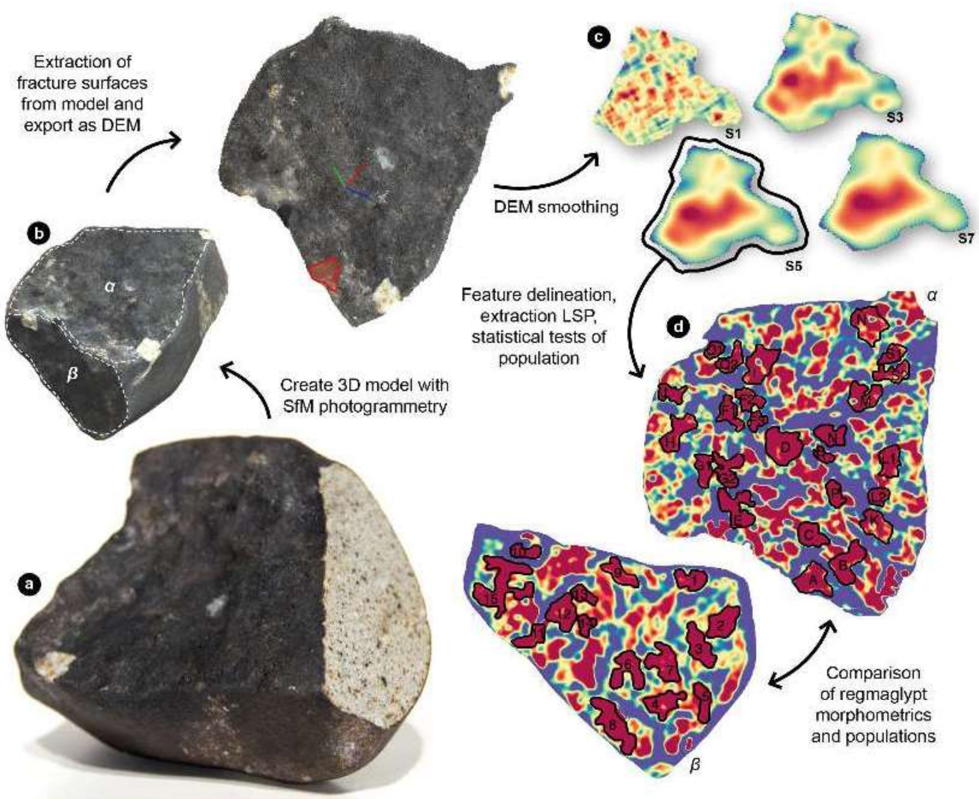

Figure 1 – Combined overview of the workflow and outcomes of this study. (a) The present state of the Broek in Waterland meteorite shown here after our photo-documentation and the sampling that took place. (b) Generated 3D model of the meteorite in its original shape shortly after recovery. (c) Mean curvature of a regmaglypt where warm colors signify larger curvatures for smoothing iterations (from left to right) 1, 3, 5 and 7. (d) Delineation of 25 regmaglypts on the large regmaglypted surface (α) and 15 regmaglypts on the small regmaglypted surface (β) of the Broek in Waterland meteorite. Red corresponds to a negative mean curvature.

are formed within a few seconds by the turbulent supersonic air stream when the velocity exceeds 10 km/s (Buchwald, 1975). When this flow regime is maintained in the denser atmospheric layers, regmaglypts can become abundant on the surface. The distribution of these surface depressions helps to determine if the object tumbled, resulting in evenly distributed equiaxial regmaglypts, or maintained a consistent attitude, resulting in elongated regmaglypts along the flight path, which can indicate the apex (Buchwald, 1975). In the latter case, a smooth surface fusion crust transitions into a surface with regmaglypts. Lin & Qun (1987) presented a physical mechanism for the formation of regmaglypts, where the surface relief is formed in a number of steps, during which the vortices generated in the ablation surface boundary layer play a major role. An example of a regmaglypted surface is that of the Broek in Waterland (L6) meteorite recovered in The Netherlands on January 11, 2017 (Figure 1a). More information about the meteorite's characteristics and recovery can be found in the initial write-up (Langbroek & Kriegsman, 2019).

Quantitative studies of a meteorite's regmaglypted surface morphology can provide insights into ablation processes and breakup events. However, literature on methods for determining the morphometrics (i.e., the quantifiable values of shapes) of surface features on meteorites is currently sparse. Teràn-Bobadilla et al. (2017) used laser scanner measurements to determine the main geometrical properties of the 4.1 m long Bacubirito meteorite (Iron-ungrouped) and its regmaglypt population. They suggested that differences found in the regmaglypt population could signify different origins of this feature (i.e., ablation processes). The potential benefits of studying the surface morphology to understand entry dynamics requires closing the gap between theoretical considerations and a practical approach. This paper therefore aims to develop an approach to study regmaglypt morphometrics and test if surfaces of the same meteorite originated from the same breakup event. As a surface study of a meteorite can be considered analogue to the analyses of land forms, we will consider methodologies commonly used for terrain analyses from geosciences that can be implemented in Geographic Information Systems. Specifically, we will extract Land Surface Parameters (LSP) from a Digital Elevation Model (DEM) that reflects the micro-topography of the meteorite surface. The objective is to find out which LSPs are a useful metric to quantify regmaglypts and compare their populations.

2 Materials and Methods

We used the Broek in Waterland (L6) as a case study to develop our methodology. The meteorite features a morphological contrast in its fusion-crusted surface: one part is well-rounded with a primary fusion crust, and it has two fracture surfaces with a secondary fusion crust that contains various regmaglypts. Our workflow progressed through various steps: (1.) Photogrammetry techniques were used to create a 3D model of the meteorite. Part of the 3D model was then selected to generate a DEM (Digital Elevation Model) that represents the height variation across the regmaglypted surfaces. (2.) The extracted DEM's were used to generate a selection of LSP's for these surfaces, and a sample of the regmaglypts on each surface was manually delineated. (3.) We then proceeded to study and select the most useful morphometrics to characterise them and find correlations between the LSP's. (4.) Finally, we evaluated the meteorite breakup event sequence. These steps will be detailed below.

Step 1: 3D shape model generation

The Broek in Waterland meteorite was imaged shortly after its recovery and before sampling took place, therefore our 3D models represent its original shape. We made use of the structure-from-motion photogrammetry implemented in the Agisoft Metashape Professional v.1.7.2 to produce a high-resolution 3D model of the meteorite[1,2]. The main mass is part of the national collection at the Naturalis Biodiversity Centre, while a virtual version of the meteorite can be viewed via the Delft Meteorite Lab (de Vet, *this issue*). Part of the 3D model data was then selected to generate a digital elevation model (DEM) in Agisoft Metashape Pro. The DEM of the largest fracture surface was used to develop the method presented here, while the smaller surface was used to study the population created by the breakup event during the final stage of our workflow. Figure 1b presents the 3D model of the larger regmaglypted surface.

Step 2: DEM preparation and LSP extraction

Surface smoothing is used to reduce the noise in the data from the DEM generation, and unnecessary surface features in analysing the regmaglypts geometry. This was done using an Edge Preserving Mean Filter of WhiteBox Tools v2.2.0 from (Lindsay, 2018), a mean filter which only includes neighbouring values within a specified threshold of the centre cell value, with a kernel of eleven pixels and threshold values of 0.15 and 0.6 for the large and small surfaces, respectively. Using the smoothed DEM, a generated a mean curvature map is generated to tune the smoothing method. The mean curvature is known as a primary regmaglypt characteristic, as depressions have a negative mean curvature. A total of five smoothing iterations (S5) were found to yield the best results without losing critical information about the surface, as shown in Figure 1c (S-i is the regmaglypt after i iterations). S1 is noisy, S3 contains unnecessary details of the surface, information on the regmaglypt shape is lost in S7, therefore S5 is selected. The outlier reduction was confirmed using boxplots of the datasets S1, S3, S5, S7 for each regmaglypt.

The Elevation Percentile (EP), slope angle, Difference From Mean Elevation (DFME), Surface Area Ratio (SA-R), Tangential Curvature (TanC), Profile Curvature (P-C), Mean Curvature (MC), Gaussian Curvature (GC), and Total Curvature (TotC) morphometrics were considered using the geospatial analysis tools from (Lindsay, 2018). The DEM's were not scaled to 'real world' physical dimensions as the study focuses on the relations between the LSP's in terms of their sign, variation across the surface, and correlations. Consequently, their absolute values do not convey meaningful information.

The next step required extracting the LSPs per regmaglypt and involved manual delineation of the regmaglypts on the two surfaces in ESRI ArcGIS Pro v2.9. Polygons were drawn based on the inflection line of the mean curvature contours, and we found that it followed the true regmaglypt shape well and produced reproducible outlines. Figure 1d shows the delineation of the regmaglypts on the larger and smaller regmaglypted surfaces where the populations are respectively labelled as (α) and (β).

Step 3: Data analysis

The most appropriate LSP's and inter-LSP's correlations describing the regmaglypts' shapes were determined based on a series of analyses performed on population α. The results were later confirmed using the population β. We used various steps and statistical tests, which we will explain here.

1. Regmaglypt outliers in the population were identified and discarded using coloured scatter plots of the mean and total curvatures, as the former is a known reliable metric for regmaglypts and the latter provides a clear graph. Outliers arise from inaccurate delineations or differences in the nature of the depression, misrepresenting the population.

2. For the LSP selection, correlations between the LSP's values and the regmaglypt surface area and depth were assessed through Pearson correlation coefficients and their two-tailed p-value. Effective morphometrics are size-independent for cross-population comparisons.

3. Also in the LSP selection, the consistency of LSP's across population α was assessed by comparing boxplots of their distribution on each regmaglypt. Good shape metrics are consistent across the population, as seen from overlapping boxes and whiskers. LSP's with large fluctuations were discarded.

[1] 3D model reconstruction [Online, accessed on 03/09/2023] https://agisoft.freshdesk.com/support/solutions/articles/31000152092

[2] Working with masks [Online, accessed on 03/09/2023] https://agisoft.freshdesk.com/support/solutions/articles/31000153479

4. To investigate LSP correlations, scatter plots with density heatmaps of the regmaglypt population were produced for all combinations of selected LSP's. The heatmap indicates representative trends of the whole regmaglypt population. Additionally, the Pearson correlation coefficient of each combination and associated p-value were obtained.

5. To select LSP correlations, the consistency of LSP correlations across population α was assessed similarly to point 3, through the distributions of Pearson coefficients for each combination.

Step 4: Comparing regmaglypt populations

We compared the regmaglypt populations on each surface using selected LSPs and their correlations to determine if they originated from the same breakup event. The correlation coefficients between the LSP's on each surface are treated as a distribution with the individual regmaglypts as data points. While the LSP distributions themselves can't be used due to different airflow exposures, if both surfaces co-evolved during the same breakup event, their airflow durations were similar, and the LSP relations within the regmaglypt populations should be alike.

The distributions of the correlation coefficients were compared using a t-test to determine if they are statistically the same. We assume that the two samples are independent with unknown but equal variances, as both distributions arose from the same physics and a similar spread in the regmaglypt data is expected. As only a few independent identically distributed random variables are available (limited number of regmaglypts), the test statistic for small sample sizes is used (Abebe, 2019; Dekking et al., 2005),

$$t = \frac{(\bar{X} - \bar{Y})}{s_p\sqrt{\frac{1}{n} + \frac{1}{m}}} \sim t_{m+n-2} \quad (1)$$

where n refers to the sample size of population α, and m refers to the sample size of population β. $\bar{X}$ is the mean of the first group, $\bar{Y}$ is the mean of the second group, and s_p is the pooled standard deviation for both groups, given by,

$$s_p = \sqrt{\frac{(n-1)s_X^2 + (m-1)s_Y^2}{n+m-2}} \quad (2)$$

where s_J for group J is given by,

$$s_J^2 = \frac{1}{\#J - 1}\sum_{i=1}^{\#J}(J_i - \bar{J})^2 \quad (3)$$

This test was applied to all selected LSP combinations with the null hypothesis H_0: the means are the same ($\bar{X} = \bar{Y}$), H_1: $\bar{X} \neq \bar{Y}$. Per convention, a p-value of 0.05 is used to determine statistical significance.

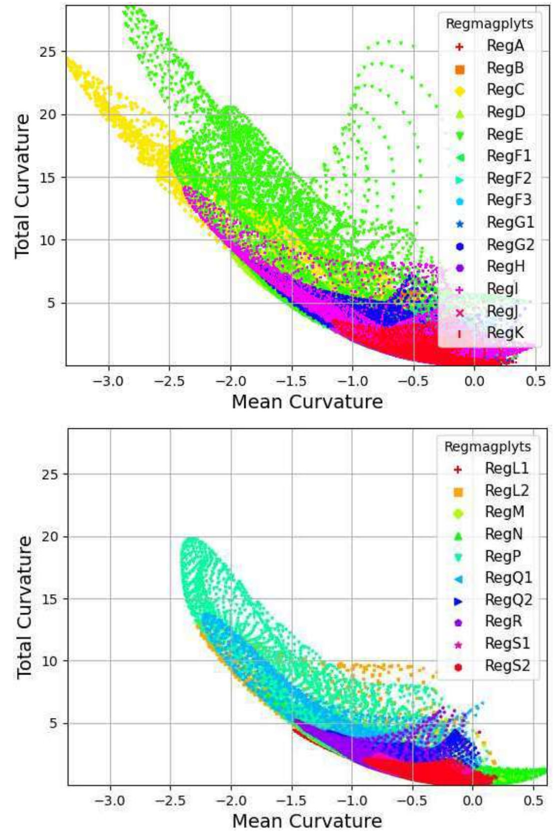

Figure 2 – Coloured scatter plots of the mean curvature and total curvature, without regmaglypt O.

3 Results and Discussion

Regmaglypt Outliers

Population outliers can skew the results of statistical tests and need to be discarded. Regmaglypt 'O' is the largest identified outlier, due to the different material present in this surface region, which leads to different ablation mechanisms. Furthermore, it is directly clear from Figure 2 that the regmaglypts C, E, and P can be considered as outliers. Those individuals are part of larger ramifications and have complex shapes making them harder to delineate. All outliers were discarded in subsequent discussions.

LSP Selection

Appropriate LSP's to describe the shape of regmaglypts need to be selected. A good morphometric is one which is consistent from one element to another and is not size-dependent, meaning that its distribution is similar across the entire population independently of the size of the regmaglypts considered. The LSP's size-dependence was assessed in the first part of Table 3 by considering the correlation between LSP mean values and the regmaglypt surface area and depth. Taking a significance threshold of 0.05, we find no statistical evidence that any of the considered surface parameters is correlated with the regmaglypts area. However, the slope, SAR, and EP are highly correlated to the regmaglypts depth. This aligns with expectations from

Table 1 – Dependence of the Land Surface Parameters on surface area, the depth of regmaglypts, qualitative description of their consistency on population α, and dependence of selected LSP's on the DFME. The table provides Pearson correlation coefficients and associated p-values, which permit to infer the shape-dependence of the regmaglypt LSP's. The last column summarises the selection results as morphometric for this study.

LSP	**Regmaglypt's surface area dependence**		**Regmaglypt's depth dependence**		**Consis -tence**	**Correlation with DFME**		**Selected?**
	Pearson. C.	*p-value*	*Pearson. C.*	*p-value*		*Pearson. C.*	*p-value*	
PC	+0.245	0.285	-0.125	0.589	Good	+0.056	0.0	Yes
DFME	+0.153	0.509	-0.248	0.279	Good	-	-	No
MC	+0.064	0.782	-0.239	0.297	Good	+0.080	0.0	Yes
GC	+0.050	0.829	+0.179	0.437	Good	-0.066	0.0	Yes
TanC	-0.100	0.668	-0.256	0.262	Good	+0.060	0.0	Yes
TotC	-0.094	0.685	+0.317	0.162	Partly	-0.069	0.0	OK
Slope	+0.053	0.818	+0.807	1E-5	Poor	-	-	No
SAR	+0.020	0.933	+0.764	6E-5	Poor	-	-	No
EP	+0.095	0.682	+0.835	2E-6	Poor	-	-	No

their definitions which are related to the local gradient. The curvature LSP's do not appear to be dependent on either the regmaglypt size or area, which indicates a common ablation process. While ablation deepens the regmaglypts, it also increases their lateral size and thus their area, resulting in similar curvatures. We speculate that this is perhaps related to the size of plasma vortices or ablation rate of the material. If this holds true, it would underpin our working premise that regmaglypt morphometrics differ depending on their ablation history.

The LSP consistency throughout the population was compared using boxplots, as shown in Figure 3 for the PC, TotC, and slope. A large variability is characterised by non-overlapping interquartile ranges from one element to another. The results for all LSP's are summarised in the second part of Table 3. Two main groups can be distinguished: (1.) great consistency across the population such as the PC, and (2.) great fluctuations from one regmaglypt to another such as the slope. The latter group is not reliable to describe regmaglypts. The Total Curvature appears to be between those groups as it is more variable than (1.) but shows much less spread than (2.) in Figure 3. However, there is insufficient reason to exclude the TotC at this point, and it is kept for subsequent analyses.

We found that the DFME produces similar distributions for both the entire surface and for its regmaglypt population, contrary to all other remaining LSP's. Furthermore, the third part of Table 3 shows that other LSP's are uncorrelated with the DFME. As it provides little additional information about regmaglypts, the DFME was discarded in subsequent analysis.

LSP Correlations

Based on the above, we found that the GC, MC, PC, TanC, and TotC are representative morphometrics of regmaglypts. A scatter plot matrix with a density heatmap of the combined population α regmaglypt data is shown in Figure 4, indicating that most regmaglypts have LSP's roughly contained within certain bounds (warm colours) and follow the same trends. Further-

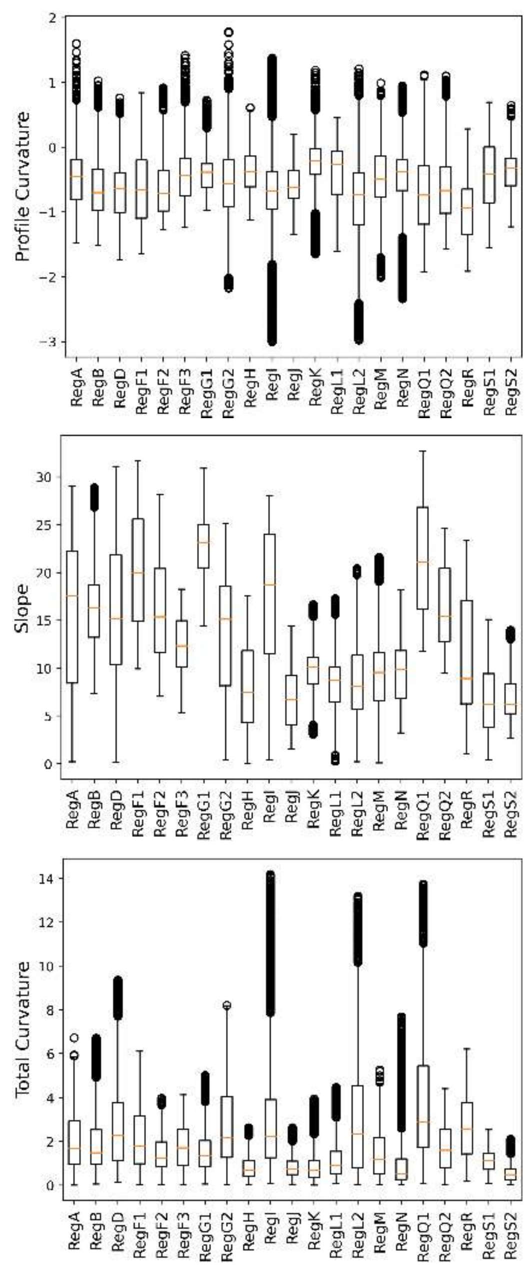

Figure 3 – Notched boxplots of the different land surface parameters for each regmaglypt.

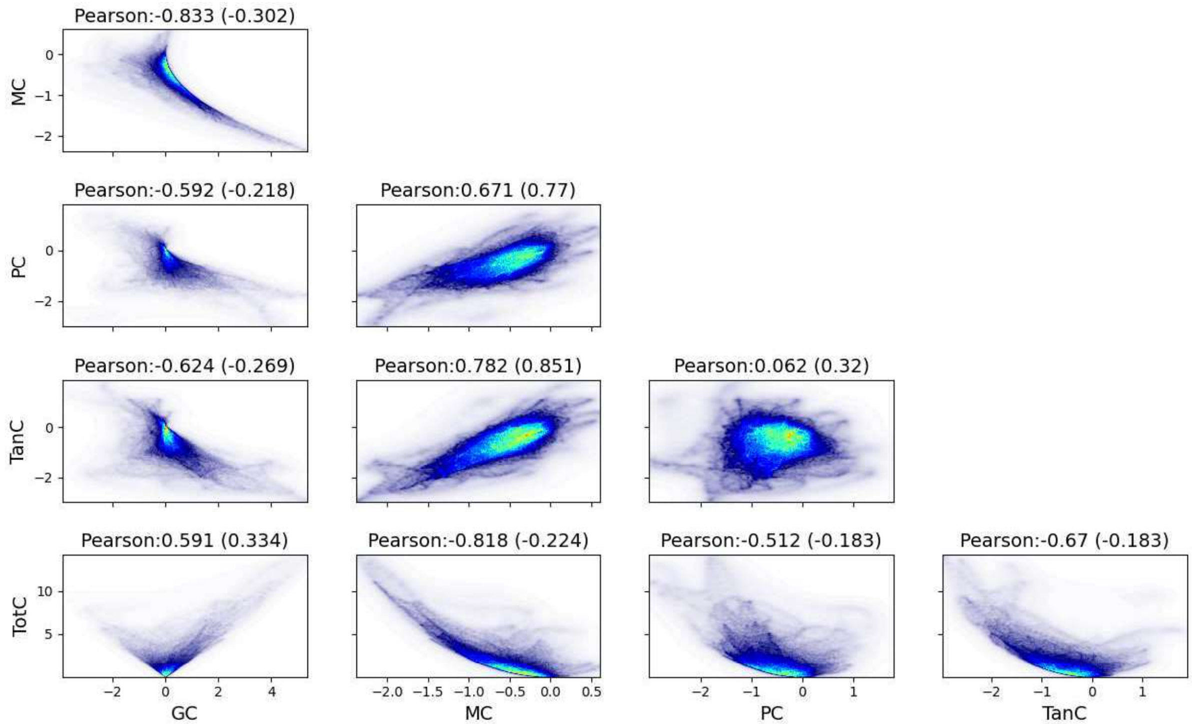

Figure 4 – Scatter plot matrix of the combined regmaglypt population α for the Gaussian, mean, profile, tangential, and total curvatures Land Surface Parameters. The heatmap highlights the denser areas of the population, permitting to distinguish representative trends. The associated Pearson correlation coefficient is provided for each combination, along its counter-part obtained from the entire large surface area (in parentheses). This permits to highlight differences between regmaglypts and the rest of the surface in terms of LSP correlations. The population was combined without scaling, meaning that larger regmaglypts have a more prominent effect on the trends observed.

more, Figure 4 shows that the Pearson correlation coefficients of the combined regmaglypt population are significantly different from the coefficients of the entire fracture surface (given between parentheses). These results indicate that specific bounds in LSP values and correlation coefficients could be used to automatically delineate regmaglypts on a fusion-crusted surface.

Similarly to the LSP selection presented in Table 3, not all LSP correlations from Figure 4 provide a reliable metric for regmaglypts. This is tackled by considering the distribution of the correlation coefficients with regmaglypts as data points. The consistency of the correlation coefficient between two LSP's was then assessed through a boxplot of the population. Correlations showing a difference larger than 0.5 between the two whiskers' ends were considered as inconsistent and were discarded, resulting in the selected LSP combinations shown in Table 2. The dominance of the MC in those results stems to two possibilities: (1.) it is indeed a primary representation of regmaglypts, (2.) bias was introduced towards the MC as it was used to delineate regmaglypts.

Breakup Event Assessment

A key motivation for this study is to better infer the conditions of breakup events of meteorites. With the selection of representative LSP correlations, we can try to assess the breakup event sequence of the Broek in Waterland by comparing the distributions of correlation coefficients between the surfaces α and β in Figure 1d.

The mean and variance of the correlation coefficient populations on each surface are given in Table 2. X refers to population α ($n = 25$) and Y population β ($m = 15$). Using the studentised distribution for $t_{40} \approx t_{38}$, a two-tailed p-value of 0.05 corresponds to 1.684 (Dekking et al., 2005). It is therefore concluded that H_0 cannot be rejected for the considered LSP combinations. This leaves two alternative hypotheses on the breakup event: (1.) the two surfaces were formed in the same breakup event, (2.) the regmaglypts arose from two breakup events but had enough exposure time to develop into a similar states. The latter implies that fracture surfaces formed in two breakup events cannot always be identified based on their regmaglypt populations.

However, video footage[3] and witness reports[4] of the fireball phase of the Broek in Waterland meteorite are available, showing no indications of multiple breakup events. This favours the first alternative hypothesis, without being able to reject the second. It is then concluded that both surfaces arose from the same breakup event, under the assumption that different exposition times to the flow results in different regmaglypt morphometrics and therefore different correlation coeffici-

[3] `https://www.youtube.com/watch?v=CayUL8kOqG8` [Accessed on 14-08-2022]

[4] `https://fireballs.imo.net/imo_view/event/2017/132` [Accessed on 14-08-2022]

Table 2 – Distribution characteristics of the Pearson correlation coefficients between selected Land Surface Parameters for population α (X) and β (Y), and associated t-test value based on Equation (1). A t-value above the 1.684 (p-value of 0.05) significance threshold implies that H_0 should be rejected.

Combination	$\bar{X}$	s_X^2	$\bar{Y}$	s_Y^2	t
MC vs GC	-0.808	0.014	-0.803	0.027	0.101
TanC vs GC	-0.564	0.034	-0.448	0.099	1.389
PC vs MC	0.656	0.006	0.61	0.020	1.267
TanC vs MC	0.697	0.018	0.720	0.009	0.575
TotC vs MC	-0.779	0.010	-0.783	0.019	0.098

ents between the LSP's.

Approach Discussion and Validity

No comparable studies on the morphometrics of regmaglypts is available in literature, offering no means for comparisons. However, following (Maxwell & Shobe, 2022), a subset of six or seven carefully selected surface parameters can provide most of the information contained in the DEM. In this work, five LSP's were shortlisted to describe regmaglypts morphometrics. This does not conflict with (Maxwell & Shobe, 2022), as some information of the surface was discarded as it does not reflect the characteristics of regmaglypts.

The method presented allows for studies of regmaglypt morphometrics to be conducted in a few hours, as only the delineation is currently done manually. Therefore, it is effective to analyse numerous meteorites of different types. Comparisons of the LSP values and correlations on regmaglypts of various meteorites, based on their compositional differences (H/L/LL), would be beneficial to draw general conclusions on the shapes of regmaglypts. Such as determining if these LSP's are a common property for L6 classes, or if they are case specific.

Furthermore, the assumption that the LSP correlations on regmaglypts strongly depend on the time of exposition to the flow requires validation, possibly by experimental studies. This can be done using wind tunnel experiments such as in (Stock & Ginoux, 1972), where regmaglyptic structures were found on wind-tunnel models used to study cross-hatched surface patterns, which are related to meteorite ablation (Larson & Mateer, 1968).

4 Conclusion and Future Work

We presented a first step towards a quantitative analysis of morphological surface features of meteorites. We conclude that use of LSP's can be extracted successfully from a DEM to study the microtopography of a meteorite. Based on the obtained results, we believe that a DEM-based approach involving terrain analysis methods commonly implemented in Geographic Information Systems (GIS) offers a potentially robust tool to extract morphometric properties. When applied to the Broek in Waterland meteorite, we found that the Gaussian, mean, total, tangential, and profile curvatures provide the best description of regmaglypts on the meteorite surface. This was in line with expectations as regmaglypts are shallow depressions best-described by their curvatures. The two regmaglypted surfaces most probably formed during the same breakup event, based on the comparison of the distribution of the Pearson correlation coefficients across the regmaglypts of each surface, using a t-test, under a p-value of 0.05 statistical significance. Continued work will help the development of our approach to further ensure robust and valid application to various regmaglypt populations. Future work needs to address other LSPs that we have not covered in this initial study, automatically delineating regmaglypts in order to help validate our working hypothesis that exposure times to the fireball plasma results in different regmaglypt morphometrics and populations. While our approach was tailored to the regmaglypts of an ordinary chondrite, we believe it will be equally relevant for other meteorite types, opening the door to broader surface-oriented studies of fusion crusts morphologies.

References

Abebe T. H. (2019). "The derivation and choice of appropriate test statistic (z, t, f and chi-square test) in research methodology". *Journal of Mathematics Letters*, **5:3**, 33–40.

Alexander C. M., Boss A., and Carlson R. (2001). "The early evolution of the inner solar system: A meteoritic perspective". *Science*, **293:5527**, 64–68.

Arrol W. J., Jacobi R. B., and Paneth F. A. (1942). "Meteorites and the age of the solar system". *Nature*, **149:3774**, 235–238.

Botines F. M. and Ernstson K. (2005). "Regmaglypts on clasts from the puerto mínguez ejecta, azuara multiple impact event (spain)".

Bouvier A. and Wadhwa M. (2010). "The age of the solar system redefined by the oldest pb–pb age of a meteoritic inclusion". *Nature Geoscience*, **3:9**, 637–641.

Buchwald V. F. (1975). *Handbook of Iron Meteorites*, volume 1. University of California Press, 45-57 pages.

Ceplecha Z. and Revelle D. O. (2005). "Fragmentation model of meteoroid motion, mass loss, and radiation in the atmosphere". *Meteoritics & Planetary Science*, **40:1**, 35–54.

Dekking F. M., Kraaikamp C., Lopuhaa H., and Meester L. (2005). *A Modern Introduction to Probability and Statistics*. Springer, London.

Langbroek M. and Kriegsman L. M. (2019). "Broek in waterland". In: Gattacceca J., Bouvier A., Grossman J., Metzler K., and Uehara M. (2019). "The meteoritical bulletin, no. 106". Meteoritics & Planetary Science, 54:2.

Larson H. and Mateer G. (1968). *Cross-hatching - A coupling of gas dynamics with the ablation process*.

Lin T. C. and Qun P. (1987). "On the formation of regmaglypts on meteorites". *Fluid Dynamics Research*, **1:3-4**, 191–199.

Lindsay J. B. (2018). *WhiteboxTools user manual*.

Maxwell A. E. and Shobe C. M. (2022). "Land-surface parameters for spatial predictive mapping and modeling". *Earth-Science Reviews*, **226**, 1–22.

Pfalzner S., Davies M. B., Gounelle M., Johansen A., Münker C., Lacerda P., Zwart S. P., Testi L., Trieloff M., and Veras D. (2015). "The formation of the solar system". *Physica Scripta*, **90:6**, 068001.

Revelle D. O. (1979). "A quasi-simple ablation model for large meteorite entry: theory vs observations". *Journal of Atmospheric and Terrestrial Physics*, **41:5**, 453–473.

Reynolds M. (2004). "Classifications of meteorites". *Journal of the Association of Lunar and Planetary Observers, the Strolling Astronomer*, **46:1**, 13–17.

Romig M. F. (1965). "Physics of meteor entry". *AIAA Journal*, **3:3**, 385–394.

Saito Y., Hong P. K., Niihara T., Miyamoto H., and Fukumizu K. (2020). "Data-driven taxonomy matching of asteroid and meteorite". *Meteoritics & Planetary Science*, **55:1**, 193–206.

Stock H. W. and Ginoux J. J. (1972). "Hypersonic low temperature ablation - an experimental study of cross-hatched surface patterns". *Astronautical Research 1971*, pages 105–120.

Takami M., Karr J. L., Hashimoto J., Kim H., Wisniewski J., Henning T., Grady C. A., Kandori R., Hodapp K. W., Kudo T., Kusakabe N., Chou M.-Y., Itoh Y., Momose M., Mayama S., Currie T., Follette K. B., Kwon J., Abe L., Brandner W., Brandt T. D., Carson J., Egner S. E., Feldt M., Guyon O., Hayano Y., Hayashi M., Hayashi S., Ishii M., Iye M., Janson M., Knapp G. R., Kuzuhara M., McElwain M. W., Matsuo T., Miyama S., Morino J.-I., Moro-Martin A., Nishimura T., Pyo T.-S., Serabyn E., Suto H., Suzuki R., Takato N., Terada H., Thalmann C., Tomono D., Turner E. L., Watanabe M., Yamada T., Takami H., Usuda T., and Tamura M. (2013). "High-contrast near-infrared imaging polarimetry of the protoplanetary disk around ry tay". *The Astrophysical Journal*, **772:2**, 145.

Terán-Bobadilla E., Abundis-Patiño J. H., Añorve C., Moraila C. R., Ortega-Gutiérrez F., and Aragón-Calvo M. A. (2017). "On a novel geometric analysis of the bacubirito meteorite". *Earth, Moon, and Planets*, **120:2**, 101–111.

Towner M. C., Jansen-Sturgeon T., Cupak M., Sansom E. K., Devillepoix H. A. R., Bland P. A., Howie R. M., Paxman J. P., Benedix G. K., and Hartig B. A. D. (2022). "Dark-flight estimates of meteorite fall positions: Issues and a case study using the murrili meteorite fall". *The Planetary Science Journal*, **3:2**, 44.

Vernazza P., Zanda B., Nakamura T., Scott E., and Russell S. (2015). "The formation and evolution of ordinary chondrite parent bodies". In *Asteroids IV*. University of Arizona Press.

Wisdom J. (1985). "Meteorites may follow a chaotic route to earth". *Nature*, **315:6022**, 731–733.

Wisdom J. (1987). "Chaotic behavior in the solar system". *Nuclear Physics B - Proceedings Supplements*, **2**, 391–414.